Hardening Mechanisms in Graphitic Carbon Nitride Films Grown with N₂/Ar Ion Assistance

R. Gago,*,† I. Jiménez,† D. Cáceres,‡ F. Agulló-Rueda,† T. Sajavaara,§
J. M. Albella,† A. Climent-Font,‖ I. Vergara,‡ J. Räisänen,⊥ and E. Rauhala§

*Instituto de Ciencia de Materiales de Madrid (CSIC), 28049 Madrid, Spain, Departamento de
Física Aplicada, Universidad Carlos III de Madrid, 28911 Leganés, Spain, Accelerator
Laboratory, University of Helsinki, P.O. Box 43, FIN-00014 Helsinki, Finland, Departamento
de Física Aplicada C-XII, Universidad Autónoma de Madrid, 28049 Madrid, Spain, and
Department of Physics, University of Jyväskylä, PB 35 (Y5), FIN-40351, Jyväskylä, Finland*

Amorphous carbon nitride films have been grown by ion beam assisted deposition (IBAD) under different process conditions. The films were found to be graphitic, with π bonds between C and N atoms and a [N]/[C] ratio below 0.3. There is a relationship between the contribution of electrons from C and N atoms to the π bonds and the mechanical properties of the films. This is consistent with the arrangement of the basal planes, the softer films consisting in the pileup of weakly interacting graphitic planes and the harder films consisting in a superstructure of interconnected and corrugated basal planes. Aiming toward the synthesis of nongraphitic hard phases, we have studied the bombardment with mixtures of nitrogen/argon ions to enhance momentum transfer in the collisions. The hardest films are obtained when using a single type of ions. The hardness is reduced in the case of the N₂/Ar mixture, indicating competitive mechanisms of cross-linking of basal planes.

1. Introduction

Carbon nitride films have been the subject of intense research since the theoretical work of Cohen and Liu predicted that the β-C_3N_4 phase would be harder than diamond.[1] Ever since, many thin film growth methods have been used to attempt the synthesis of this phase. Although the formation mechanism of β-C_3N_4 is still unclear, many carbon nitride films grown have presented good mechanical properties, including high elasticity and hardness values of ~20 GPa for films with low nitrogen contents[2] and up to ~60 GPa for films with higher nitrogen concentrations.[3] These features have considerably stimulated the study of amorphous carbon nitride films.

The nitrogen content in the carbon nitride films, normally limited below 50 at. %,[4−6] has been considered the main parameter affecting the physical properties of the films. However, the amount of N incorporated is not

a good measure of the film quality, since similar N contents may lead to very different film properties, depending on the growth process used. The bonding structure is, hence, the main parameter controlling the physical properties. Relating the deposition parameters with the film properties and bonding structure is, therefore, of major importance.

Most of the results on the synthesis of carbon nitride films are consistent with the existence of four different bonding structures. The first possible structure is the β-C_3N_4 phase with theoretical extreme hardness, which is based on σ bonds between sp³ carbon hybrids and sp² nitrogen. Only a few reports are consistent with the synthesis of β-C_3N_4 nanocrystals embedded in an amorphous matrix, making difficult a clear characterization of the actual material.[7] A second possible structure consists of a network of sp³ carbon atoms, capable of accommodating a certain amount of substitutional nitrogen. The tetrahedral carbon network is stable for a nitrogen doping < 10 at. %,[8] transforming into a graphitic structure beyond that value with a substantial hardness decrease.[9] The third possibility consists of a polymeric structure containing a large proportion of C≡N bonds.[10,11] In this case, the hardness decreases with the nitrogen content. Finally, the fourth structure

* Corresponding author: Telephone: 34 91 334 90 00. Fax: 34 91 372 06 23. E-mail: rgf@icmm.csic.es.
† Instituto de Ciencia de Materiales de Madrid (CSIC).
‡ Universidad Carlos III de Madrid.
§ University of Helsinki.
‖ Universidad Autónoma de Madrid.
⊥ University of Jyväskylä.

(1) Liu, A. Y.; Cohen, M. L. *Science* **1989**, *245*, 841.
(2) Kohzaki, M.; Matsumuro, A.; Hayashi T.; Muramatsu, M.; Yamaguchi, K. *Thin Solid Films* **1997**, *308−309*, 239.
(3) Sjöström, H.; Strafström, S.; Boman, M.; Sundgren, J. E. *Phys. Rev. Lett.* **1995**, *75* (7), 1336.
(4) Ronning, C.; Feldermann, H.; Merk, R.; Hofsäss, H.; Reinke, P.; Thiele, J. U. *Phys. Rev. B* **1998**, *58*, 2207.
(5) Merchant, A. R.; McCulloch, D. G.; McKenzie, D. R.; Yin, Y.; Hall, L.; Gerstner, E. G. *J. Appl. Phys.* **1996**, *79*, 6914.
(6) Holloway, B. C.; Shuh, D. K.; Kelly, M. A.; Tong, W.; Carlisle, J. A.; Jimenez, I.; Sutherland, D. G. J.; Terminello, L. J.; Pianetta P.; Hagstrom, S. *Thin Solid Films* **1996**, *290/291*, 94.

(7) Yamamoto, K.; Koga, Y.; Yase, K.; Fijiara, S.; Kubota, M. *Jpn. J. Appl. Phys. Part 2*, **1997**, *36*, L230.
(8) Hu, J.; Yang, P.; Lieber, C. M. *Phys. Rev. B* **1998**, *57*, R3185.
(9) Liu, E.; Shi, X.; Tan, H. S.; Cheah, L. K.; Sun, Z.; Tay B. K.; Shi, J. R. *Surf. Coat. Technol.* **1999**, *121*, 601.
(10) Ng, Y. M.; Ong, C. W.; Zhao X. A.; Choy, C. L. *J. Vac. Sci. Technol. A* **1999**, *17* (2), 584.
(11) Chowdhury, A. K. M. S.; Monclus, M.; Cameron, D. C.; Gilvarry, J.; Murphy, M. J.; Barradas, N. P.; Hashmi, M. S. *J. Thin Solid Films* **1997**, *308−309*, 130.

is based in a graphitic network with substitutional nitrogen in the hexagonal rings, whose hardness increases with the nitrogen content.[12,13]

In this work we study the structure and hardness of carbon nitride films grown by ion beam assisted deposition (IBAD), using graphite evaporation and bombardment with a mixture of N_2 + Ar ions. The results are compared with those from a previous study on samples grown with 100% N_2 assistance.[14] The films are graphitic and belong to the fourth category described above. Bombardment with mixtures of nitrogen and argon ions was performed, aiming toward the synthesis of harder materials with sp^3 carbon hybrids. It is well-established in the synthesis of tetrahedral carbon and tetrahedral BN films that one needs the assistance of heavy noble ions to increase the momentum transfer in the collisions, promoting the formation of sp^3 hybrids.[15,16] However, we found that for graphitic CN_x the hardness is reduced in the case of the N_2/Ar gas mixture, indicating that film hardening by promotion of C-sp^3 hybrids is a competitive process with hardening by nitrogen incorporation.

2. Experimental Section

2.1. Film Preparation. The thin film growth system used in this work has been described elsewhere.[17] The a-CN_x films were obtained by electron-beam evaporation of graphite lumps with concurrent ion bombardment from a N_2/Ar discharge. The films were grown on p-type (100) oriented Si substrates ultrasonically cleaned with acetone and dried up with N_2. Further cleaning was performed with 300 eV Ar^+ sputtering for 2 min prior to deposition.

Graphite was evaporated with an electron gun at a rate of ∼3 Å/s. The power density applied in the evaporation was 825 W/cm². The ion beam assistance was performed with a Kauffman-type ion gun with a beam diameter of 3 cm. The ion gun voltage and current were varied between 0 and 500 V and 0 and 15 mA, respectively. With these growth parameters and with the assumptio of a typical ion beam composition for nitrogen (90% N_2^+ and 10% N^+),[18] the transport ratio (TR) of nitrogen or argon ions reaching the surface ranged between 0 and 12. Since the films were grown typically with TR ≫ 1 and the nitrogen content in the films was always below 20 at. %, it is clear that the reactivity of nitrogen with carbon, forming volatile species, affects largely the growth rate.[19]

2.2. Film Characterization. Film thickness was determined with a Dektak 3030 profiling system. The measurement was performed from the step created by locating a mask during deposition in front of the substrate. The process was repeated four times on different points, and the average value was taken as the final result, giving the film thickness with an accuracy of 10%.

Time-of-flight elastic recoil detection analysis (TOF-ERDA)[20] was performed with the 5 MV tandem accelerator EGP-II at the Accelerator Laboratory of the University of Helsinki. The experiments were performed with an incident beam of 48 MeV

I^{+9} and the recoils were detected at a scattering angle of 40°. This technique is very useful for the detection of light elements. In the experiment, the kinetic energy and velocity are measured simultaneously, which allows the determination of the mass of the recoil. Thus, it is possible to separate the spectrum for each mass practically clean from unwanted background or interference from other signals. This feature is of great help in the evaluation of the concentration depth profiles.

X-ray photoelectron spectra (XPS), excited with Mg Kα radiation, were acquired with a double pass cylindrical mirror analyzer (Physical Electronics). The overall instrumental energy resolution is ∼0.8 eV. The spectrometer is calibrated with the Au(4f)$_{7/2}$ peak at 83.8 eV of binding energy, the C(1s) peak from crystalline graphite appearing at 284.5 eV.

X-ray absorption near-edge spectroscopy (XANES) measurements were performed at the SACEMOR end-station (beam line SA72) of the Laboratoire pour L'Utilisation du Rayonnement Electromagnetique (LURE). The data were acquired in the total yield mode by collecting the electron emission from the sample with a channeltron. The signal was normalized to the photocurrent obtained from a gold-covered grid, recorded simultaneously.

Micro-Raman spectra were collected with a Renishaw Ramascope 2000 microspectrometer at an excitation wavelength of 514.5 nm. The power density on the sample was about 5 GW/m². The spectral resolution achieved with this system is 1 cm^{-1}, and the spectral slit width is 4 cm^{-1}. The spectra were acquired between 0 and 4000 cm^{-1} in order to see bands associated with the C−N bonding apart from the first-order C=C band between 1000 and 2000 cm^{-1}.

Nanoindentation experiments were made using a Nano Indenter II (Nano Instruments, Inc). To obtain the hardness and elastic modulus, the indenter was loaded and unloaded at increasing depths at a constant rate of 10% of the maximum depth per second. Each unloading was terminated at 10% of the peak load to ensure that the contact was maintained between the specimen and indenter. Hold periods of 10 s at the maximum loads and 100 s at the minimum load of the final unloading were inserted to correct creep and thermal drift effects, respectively. The load−displacement data obtained were analyzed using the method of Oliver and Pharr.[21] Each indentation experiment was performed 10 times in each sample, and the mean value of hardness was adopted as the result of the measure. The dispersion is always below 8%, which can be considered as the error of the hardness for a certain depth.

3. Results and Discussion

3.1. Film Composition. The nitrogen content is an important characterization parameter, commonly used to classify the CN_x films. We have checked the lateral and transversal homogeneity of our films by determining the composition at different points of each film and by using techniques with different depth sensitivities, respectively. In this context, the film composition was measured by X-ray photoemission spectroscopy (XPS), X-ray absorption spectroscopy (XAS or XANES), and time-of-flight elastic recoil detection analysis (TOF-ERDA). The results from the different techniques are consistent with a dispersion of 15−20%, depending on the sample. The N content presented throughout this work corresponds to the XANES data.

In the XPS measurements, electrons from the whole film area (∼1 cm²) were collected. The nitrogen fraction (X = [N]/[C]) was computed from the relative intensity of the N(1s) and C(1s) core level spectra, corrected for

(12) Souto, S.; Pickholz, M.; dos Santos, M. C.; Álvarez, F. *Phys. Rev. B* **1998**, *57*, 2536.

(13) Hellgren, N.; Johansson, M. P.; Broitman, E.; Hultman, L.; Sundgren, J. E. *Phys. Rev. B* **1999**, *59*, 5162.

(14) Jiménez, I.; Gago, R.; Albella, J. M.; Cáceres, D.; Vergara, I. *Phys. Rev. B* **2000**, *62*, 4261.

(15) Kester, D. J.; Messier, R. *J. Appl. Phys* **1992**, *72* (2), 504.

(16) Rossi, F.; Andrè, B.; van Veen, A.; Mijnaredns, P. E.; Schut, H.; Delplancke, M. P.; Gissler, W.; Haupt, J.; Lucazeau, G.; Abello, L. *J. Appl. Phys.* **1994**, *75*, 3121.

(17) Gago, R.; Böhme, O.; Albella, J. M.; Román, E. *Diamond Relat. Mater.* **1999**, *8*, 1944.

(18) Hammer, P.; Gissler, W. *Diamond Relat. Mater.* **1996**, *5*, 1152.

(19) Gago, R.; Jiménez I.; Albella, J. M. *Thin Solid Films*, in press.

(20) Withlow, H. J.; Possnert, G.; Petersson, C. S. *Nucl. Instrum. Methods Phys. Res., Sect. B* **1997**, *27*, 448.

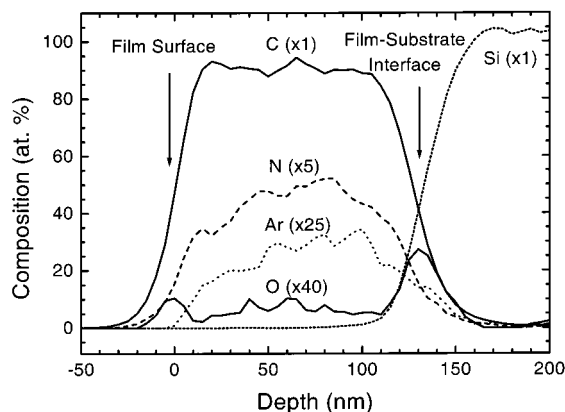(21) Oliver, W. C.; Pharr, G. M. *J. Mater. Res.* **1992**, *7−6*, 1564.

Figure 1. TOF-ERDA composition depth profile of a carbon nitride film grown by IBAD (91% N_2 and 9% Ar in the gas mixture, 360 eV and 7.5 mA). The density used in the analysis was 2.33 g/cm^3.

the atomic sensitivity factor.[22] XPS is a conventional technique for composition analysis with an analysis depth of ~2 nm.

XANES analyzes the area of the synchrotron spot size, in our case, ~1 mm^2. The measurements were repeated in several points of each sample with identical results. XANES provides more detailed information about the bonding structure than XPS, with an analysis depth of ~10 nm. The computation of the N content is performed from the relative height of the N(1s) respect to the C(1s) absorption edges, corrected with a proportionality factor determined from comparison with reference crystalline h-BN and B_4C samples. We have found that the proportionality factor depends on the cleanliness of the grid used for signal normalization. Therefore, in situ calibration with reference samples is preferred to the use of tabulated absorption cross-sections.

The TOF-ERDA analysis area is ~10 mm^2. In this case, all the depth profiles through the film can be obtained in a single experiment. Figure 1 shows the composition profile obtained with TOF-ERDA of a sample grown with 91% N_2 and 9% Ar ion assistance, 360 eV and 7.5 mA. The shape of the profile indicates that nitrogen atoms are distributed over the whole film thickness, within a concentration variation of ~20%. The hydrogen content is below 1 at. % for all the films measured, and it is not shown in the figure. The oxygen signal is detected at the film−substrate interface with a content of ~0.5 at. % and at the film surface with a content of ~0.25%. The oxygen concentration in the bulk of the film falls below 0.25 at. %.

Figure 2 shows in panel a the nitrogen content measured with XANES and in panel b the deposition rate as a function of the ion energy at fixed current (solid dots) and ion current at fixed energy (open dots) for samples grown with nitrogen assistance. The nitrogen fraction is below 0.3 in all cases. The ion energy is the main parameter affecting the nitrogen content and the deposition rate. The reduction of the deposition rate is a consequence of the physical resputtering and formation of C−N volatile compounds induced by the nitrogen ions.[19] With regard to the ion current, the nitrogen content reaches quickly a saturation value of [N]/[C] =
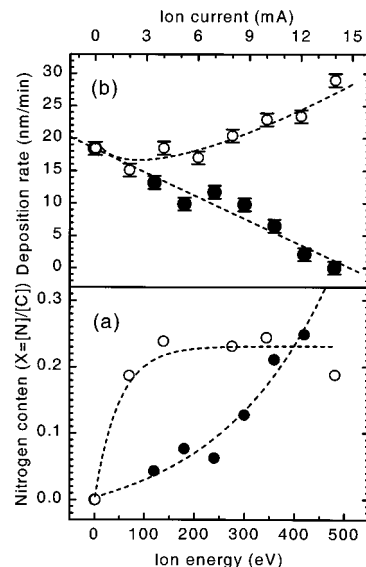

Figure 2. Nitrogen content measured with XANES (a) and deposition rate (b) as a function of the assisting ion energy (100% N_2, 10 mA) (solid dots) and current (100% N_2, 360 eV) (open dots).
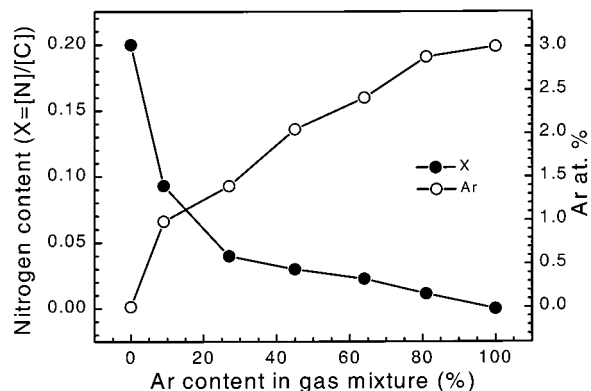

Figure 3. Nitrogen fraction (X = [N]/[C]) and Ar content measured with TOF-ERDA for a set of samples grown with different N_2/Ar gas mixtures (360 eV, 7.5 mA).

0.3 without further variations, and the deposition rate increases slightly with the ion current. This behavior implies that the increase of the number of reactive nitrogen ions reaching the substrate at a constant ion energy favors the formation of carbon nitride, but does not increase the nitrogen uptake into the material. There is an intrinsic limitation of [N]/[C] = 0.3 in the deposition method, which seems to be related to the volatility of CN_x nitride moieties with larger nitrogen contents formed during the film growth.[23,24]

Figure 3 displays the composition for a set of samples grown with different Ar/N_2 gas mixtures, as determined from TOF-ERDA measurements. The Ar content incorporated in the film shows a saturation value of 3 at. %, identical to that found in amorphous carbon films.[17,25] The N content incorporated decreases with the Ar content in the gas mixture. This decrease is nonlinear and can be attributed to two different factors: first, the

(22) *Handbook of X-ray Photoelectron Spectroscopy*; Perkin-Elmer Corporation: Minnesota, USA, 1979.

(23) Hammer, P.; Gissler, W. *Diamond Relat. Mater.* **1996**, *5*, 1152.
(24) dos Santos, M. C.; Álvarez, F. *Phys. Rev. B* **1998**, *58*, 13918.
(25) Gago, R.; Jiménez, I.; Albella, J. M.; Climent-Font, A.; Cáceres, D.; Vergara, I.; Banks, J. C.; Doyle B. L.; Terminello, L. J. *J. Appl. Phys.* **2000**, *87*, 8174.
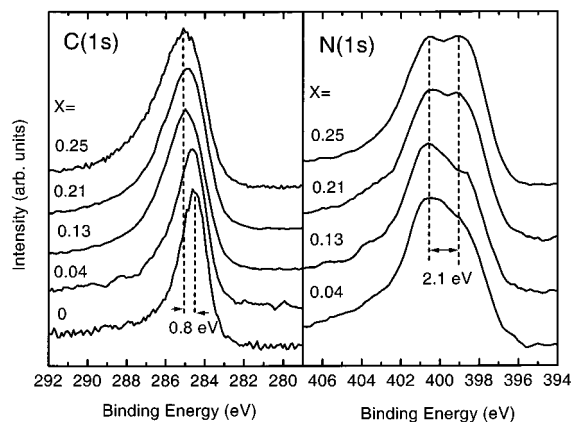
Figure 4. C(1s) (left panel) and N(1s) (right panel) core level photoemission spectra for a set of samples with different nitrogen content.

reduction of the number of incident nitrogen ions in the assisting beam; second, the breakage of polar C−N bonds upon Ar$^+$ bombardment and preferential sputtering of carbon nitride areas. A small decrease of the deposition rate with increasing Ar contents takes place, supporting the consideration of the last argument.

3.2. Bonding Structure. Figure 4 shows the C(1s) and N(1s) photoemission spectra for a series of samples with increasing nitrogen content. The C(1s) spectra appears as a single peak that broadens and moves toward higher binding energies with increasing nitrogen content. This trend results from charge transfer from the carbon atoms to the more electronegative nitrogen atoms. The centroid of the curve shifts ∼0.8 eV over the composition range considered, without any resolvable component. The N(1s) spectra are apparently composed of two peaks separated ∼2.1 eV. The intensity of the low-binding-energy peak increases with increasing nitrogen contents, in agreement with previous results. There is a discrepancy in the literature about the interpretation of the two N(1s) peaks, since some experimental and theoretical works assign the low-binding-energy peak to sp^3 hybridized nitrogen,[26] while other reports indicate that both peaks correspond to sp^2 hybridized N forming π bonds.[27]

Our results are similar to previous XPS reports of amorphous carbon nitride films,[12] similar to the XPS data from samples claimed to have a certain proportion of the β-C$_3$N$_4$,[28] and similar to very elastic samples claimed to contain nitrogen with 4-fold coordination compatible with the graphitic matrix.[29] Further information cannot be derived from the XPS data regarding either different coordination or different hybridization, since both factors affect the energy shifts. Instead, we have performed an XANES study finding a dominant proportion of π bonding, hence, corresponding to a graphitic network.

Figure 5 shows the C(1s) and N(1s) XANES spectra from selected carbon nitride films together with references from highly oriented pyrolitic graphite (HOPG),

diamond, hexagonal BN, and cubic BN, as prototype materials with sp^2 and sp^3 hybridization. The spectra are shown normalized to the same height. The energy scale of the C(1s) spectra is referenced to the π^* resonance from HOPG at 285.4 eV, and that of the N(1s), to the π^* resonance from h-BN at 400.9 eV.[30] Sample #A is a carbon film evaporated without ion assistance, with a ∼95% sp^2 C content. Samples #B and #C are carbon nitride films with different N contents, grown with 100% N$_2$ ion assistance. Sample #D is a CN$_x$ film grown with ion assistance from a gas mixture of 73% N$_2$ + 27% Ar, and sample #E, with a gas mixture of 55% N$_2$ + 45% Ar. Sample #F is an amorphous carbon film grown with 100% Ar$^+$ assistance, containing ∼30% sp^3 hybrids.[25] The corresponding [N]/[C] ratios are indicated in the figure.

The shape of the C(1s) edge for all the carbon nitride films resembles the spectrum from the amorphous carbon film #A. The presence of C−N bonds of π^* character is revealed by the appearance of several peaks in the 286−289 eV region. Six different features can be resolved in the C(1s) spectra. Peaks C1 and C2 are related to distorted graphitic bonding in amorphous carbon,[25] peaks C3, C4, and C5 correspond to different C−N π bonds,[6,31,32] and peak C6 seems related to surface contamination, presumably of C=O type, since its intensity appears related to the oxygen signal.[25] The amorphous carbon samples #A and #F do not show intense peaks C3, C4, and C5. The ∼30% C sp^3 content in sample #F is reflected in a lower intensity of π^* states between 283 and 289 eV compared to sample #A.

The N(1s) spectra of carbon nitride samples contain three well-resolved peaks in the 396−402 eV range, indicating π^* bonding in three different chemical environments. This three peak structure has been observed by other groups[27,33,34] and seems typical of carbon nitride films with an [N]/[C] ratio < 0.4. For higher nitrogen contents, the N(1s) XANES contains a single broad π^* peak[6,31] that can be understood from the merging of the three peaks observed here for low nitrogen concentrations.[32]

When N$_2$/Ar gas mixtures are used for ion assistance, the relative intensity of C−N peaks is affected. For instance, sample #E shows in the C(1s) spectrum a dominant peak C3 and in the N(1s) a dominant peak N2 with a clear decrease of peak N3. However, the actual atomic arrangement yielding the different peaks is still unknown.

Additional information can be extracted from the XANES spectra by studying the contribution of electrons from the C and N atoms to the π bonds, computing the intensity of the π^*-state region relative to the total absorption intensity in the C(1s) and N(1s) spectra, as has been described in detail in ref 14 for samples grown

(26) Johansson Å.; Stafström, S. *J. Chem. Phys. B* **1999**, *111*, 3203.

(27) Ripalda, J. M.; Román, E.; Díaz, N.; Galán, L.; Montero I.; Gomelli, G. *Phys. Rev. B* **1999**, *60,* R3705.

(28) Marton, D.; Boyd, K. J.; Al-Bayati, A. H.; Todorov, S. S.; Rabalais, J. W. *Phys. Rev. Lett.* **1994**, *73* (1), 118.

(29) Holloway, B. C.; Kraft, O.; Shuh, D. K.; Kelly, M. A.; Nix, W. D.; Pianetta P.; Hagström, S. *Appl. Phys. Lett.* **1999**, *74*, 3290.
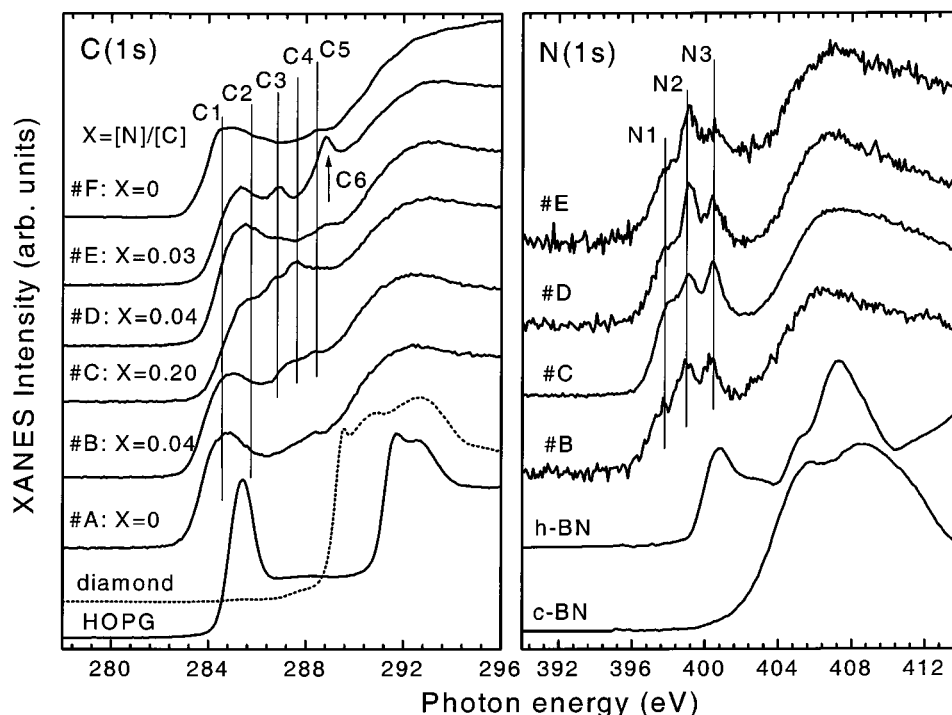
(30) Jiménez, I.; Jankowski, A. F.; Terminello, L. J.; Carlisle, J. A.; Sutherland, D. G. J.; Doll, G. L.; Tong, W. M.; Shuh, D. K.; Himpsel, F. J. *Phys. Rev. B* **1997**, *55*, 12025.

(31) López, S.; Dunlop, H. M.; Benmalek, M.; Tourillon, G.; Wong M. S.; Sproul, W. D. *Surf. Interface Anal.* **1997**, *25*, 827.

(32) Jiménez, I.; Tong, W. M.; Shuh, D. K.; Holloway, B. C.; Kelly, M. A.; Pianetta, P.; Terminello, L. J.; Himpsel, F. J. *Appl. Phys. Lett.* **1999**, *74*, 2620.

(33) Quirós, C.; Núñez, R.; Prieto P.; Vergara, I.; Cáceres, D.; Soriano, L.; Fuentes, G. G.; Elizalde, E.; Sanz, J. M. *Surf. Coat. Technol.* **2000**, *125*, 284.

(34) Lübbe, M.; Park, S.; Bressler, P. R.; Braun, W.; Zahn, D. R. T. *BESSY;* Jahresbericht: Berlin, Germany, 1998; p 378.

Figure 5. C(1s) (left panel) and N(1s) (right panel) XANES spectra for selected samples: #A, evaporated carbon film with ~95% sp^2 C; #B and #C, carbon nitride films grown with 100% N$_2$ ion assistance; #D, CN$_x$ film grown with ion assistance from a gas mixture of 73% N$_2$ + 27% Ar; #E, CN$_x$ film grown with ion assistance from a gas mixture of 55% N$_2$ + 45% Ar, #F, amorphous carbon film grown with 100% Ar$^+$ assistance containing ~30% sp^3 C.
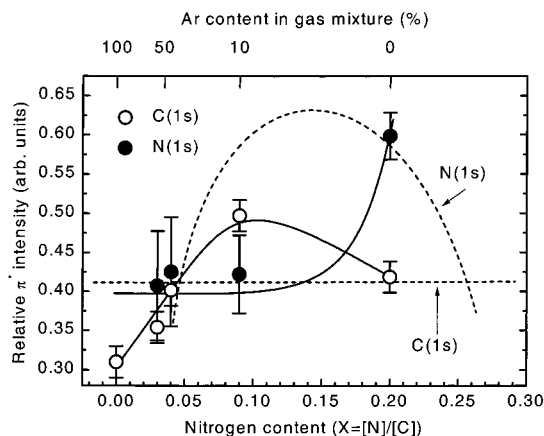

Figure 6. XANES relative intensity of π^* respect to σ^* states for the C(1s) (open dots) and N(1s) (solid dots) edges for different N$_2$/Ar mixtures as a function of the nitrogen content. The dashed lines correspond to the behavior for 100% N$_2$ assistance (from ref 14).

with 100% N$_2$ ion assistance. In Figure 6 we compare the results from ref 14, shown with dashed lines, with those from the samples grown with N$_2$ + Ar gas mixtures, represented with dots. The solid lines represent the trends found for the samples grown with gas mixtures. A different behavior is found for both sets of samples.

The samples grown with 100% N$_2$ ion assistance (dashed lines) show a constant density of carbon π^* states, and a variation of density of nitrogen π^* states with a maximum at [N]/[C] ~ 0.15. The relative C(1s) π^* intensity remains the same as for an evaporated carbon film, which implies an sp^2 carbon content ~ 95%.[17,25] The increase of the N(1s) π^* intensity for $X <$ 0.15 is explained by a transition from nonplanar to

planar nitrogen bonding geometry,[14] since conjugation of the nitrogen p electrons with the hexagonal ring will be maximum for flat basal planes.[35] The most planar configuration occurs for one substitutional nitrogen per hexagonal ring in the graphitic network, which corresponds to the threshold value of $X \sim$ 0.15. The decrease for $X >$ 0.15 is explained by an increased corrugation of the basal planes,[24] with eventual cross-linking through nitrogen atoms.[14,29]

The samples grown with Ar in the gas mixture show a constant density of π^* states from nitrogen, indicating that changes in the corrugation of basal planes are not taking place. A plausible explanation stems from the breakage of graphitic planes into small fragments or the presence of a large vacancy concentration in the graphitic planes due to the Ar$^+$ bombardment. In this case, the stress introduced by N insertion in hexagonal rings is released without changes of corrugation in the basal planes. This argument is also supported by the Raman microstructural information presented in the next section.

Finally, the samples obtained with more than 50% Ar in the gas mixture show the formation of carbon sp^3 sites as evidenced by the decrease of the C(1s) π^* intensity.

3.3. Microstructure. The cross-linking of graphitic planes must reflect in the microstructure of the films, which can be studied by Raman spectroscopy. This technique is sensitive to the grain size in nanometric and amorphous graphitic films.[36,37] Figure 7 shows the visible Raman spectra for the samples considered in

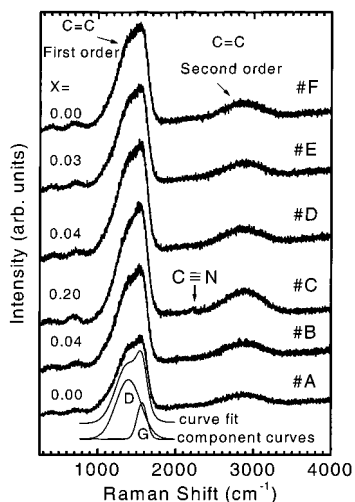(35) McWeeny, R. *Coulsons Valence*; Oxford University Press: Oxford, U.K., 1979.

Figure 7. Visible Raman spectra for the samples considered in Figure 5.

Figure 5 and described in the preceding section. The graphitic structure of the carbon nitride films is evidenced by the similar spectral line shape to the amorphous carbon film #A. The band around 690 cm^{-1} is due to C−C vibrations out of the basal planes that only occur when there is structural disorder in the graphitic network.[38,39] The bands between 1000 and 2000 cm^{-1} and 2500−3500 cm^{-1} correspond to the first- and second-order Raman spectrum of disordered sp^2 carbon, respectively. The presence of a small nitrile (C≡N) feature around 2200 cm^{-1} is only found for nitrogen fractions over 0.1. A prominent nitrile band (not our case) is typical of polymeric paracyanogen-like film.[10]

To obtain information about the microstructure of the films, the first-order band of the carbon stretching mode between 1000 and 2000 cm^{-1} was fitted with a linear background and two Gaussian distributions, labeled "G" (graphite) and "D" (disorder). This analysis is similar to what is done in the study of amorphous carbon.[25,40] The position, width, and relative intensity of these peaks are found to vary systematically with deposition conditions and film properties.[41,42] The results of the fitting analysis are shown in Figure 8. The black dots correspond with samples grown with 100% N$_2$ ion assistance and the white dots with ion assistance with Ar + N$_2$ gas mixtures.

First, we describe the effect of nitrogen incorporation for samples grown with 100% N$_2$ ion assistance. For evaporated carbon without assistance, the position of the G peak in panel a is around 1575 cm^{-1} and close to the crystalline graphite value (1580 cm^{-1}). With increasing nitrogen content, the G band shifts toward lower frequencies, indicating a distortion of the graphitic
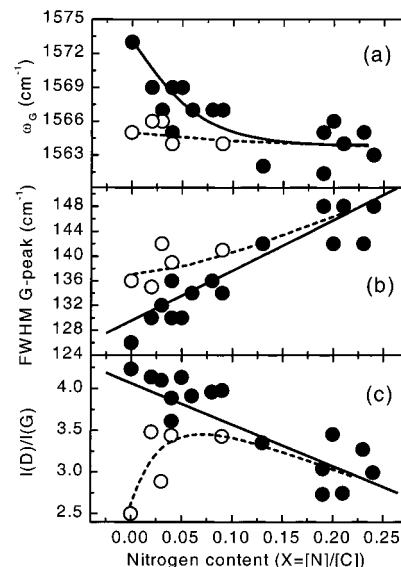

Figure 8. Fitting parameters of the Raman spectra as a function of the nitrogen fraction: Position of the G peak (a), full width at half-maximum (fwhm) of the G peak (b), and relative intensity of the D and G peaks (c). Black dots represent samples grown with 100% N$_2$ ion assistance and white dots with Ar + N$_2$ assistance.

network.[43] Figure 8 also shows the width of the Raman peak G in panel b and the relative intensity $I(D)/I(G)$ in panel c. The incorporation of nitrogen induces the widening of the G peak and the decrease of the $I(D)/I(G)$ ratio, indicating an amorphization of the graphite network. These results indicate a distortion of the graphitic network and a decrease of the graphitic domain size with increasing nitrogen contents. This behavior is consistent with the cross-linking of graphitic planes through nitrogen atoms.

Regarding the samples grown with Ar + N$_2$ gas mixtures, the data in Figure 8 indicate that the degree of amorphization is larger than what corresponds to their nitrogen content. This effect is due to the additional Ar$^+$ bombardment, which in principle can contribute to both promotion of C sp^3 hybrids and breakage of the graphitic network by creation of defects. Comparison with the mechanical properties of the samples indicates which is the effect of the Ar$^+$ bombardment.

3.4. Mechanical Properties. We have determined by nanoindentation experiments the elastic modulus (E) and hardness (H) of our films. We have found that they follow well the rule $E/H \sim 10$ and, therefore, we only consider the hardness values in the discussion. Figure 9 shows the hardness values obtained as a function of the argon content in the gas mixture. The nitrogen content of the films is shown in the scale of the top *x*-axis.

The dashed line corresponds to the dependence found for samples grown with 100% N$_2$ assistance, described in ref 14. In that case, the incorporation of nitrogen to the graphitic network produces a film hardening, mostly for [N]/[C] above a threshold value of ~0.15. That behavior is explained by the cross-linking of basal planes for nitrogen content above 0.15, consistently with

(36) Tuinstra, F.; Koenig, J. L. *J. Chem. Phys.* **1970**, *53*, 1126.
(37) McCulloch, D. C.; Prawer S.; Hoffman, A. *Phys. Rev. B* **1994**, *50*, 5905.
(38) Parmigiani, F.; Kay, E.; Seki, H. *J. Appl. Phys.* **1988**, *64*, 3031.
(39) Chen, M. Y.; Li, D.; Lin, X.; Dravid, V. P.; Chung, Y.; Wong, M.; Sproul, W. D. *J. Vac. Sci. Technol. A* **1993**, *11* (3), 521.
(40) Dillon, R. O.; Woollam, J. A.; Katkanant, V. *Phys. Rev. B* **1984**, *29*, 3482.
(41) Tamor, M. A.; Vassell, W. C. *J. Appl. Phys.* **1994**, *76*, 3823.
(42) Prawer, S.; Nugent, K. W.; Lifshitz, Y.; Lempert, G. D.; Grossman, E.; Kulik, J.; Avigal, I.; Kalish, R. *Diamond Relat. Mater.* **1996**, *5*, 433.

(43) Beeman, D.; Silverman, J.; Lynds R.; Anderson, M. R. *Phys. Rev. B* **1984**, *30*, 870.
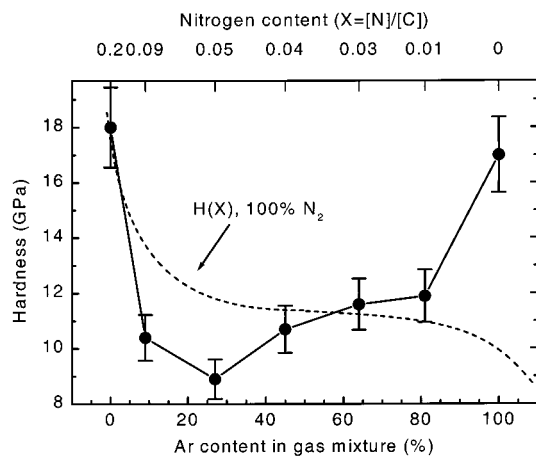
Figure 9. Hardness of a set of samples grown with different argon contents in the N_2/Ar gas mixture (360 eV, 7.5 mA). The dashed line corresponds with the behavior for 100% N_2 ion assistance (from ref 14).

the development of the XANES density of π^* states shown in Figure 5. Since the density of π^* states in the C(1s) edge remains constant, hardening by formation of sp^3 carbon hybrids is excluded.

Regarding the samples grown with Ar + N_2 ion assistance, those with less than 50% Ar in the gas mixture are softer than would correspond to samples grown without Ar. This indicates that Ar bombardment is not promoting sp^3 sites but is disrupting the graphitic network by defect creation. However, for Ar contents in the gas mixture above 50% the samples are harder than would correspond to their nitrogen content. In this last case, the hardness increase is directly related to the formation of carbon sp^3 sites as evidenced by the decrease of the C(1s) π^* intensity in Figure 6.

It is noteworthy that similar hardness values are obtained for CN_x films with a nitrogen content of ~20 at. % and for an amorphous carbon film with a similar sp^3 content. In both cases the proposed hardening mechanism is the same, i.e., cross-linking of graphitic planes, but through different linking sites: nitrogen atoms for CN_x films and sp^3 carbon atoms for amorphous carbon films. The hardening mechanisms of cross-linking through N atoms and C-sp^3 hybrids are competitive, since the samples grown with intermediate Ar/ N_2 values in the gas mixture are softer.

4. Conclusions

Carbon nitride films grown by carbon evaporation with N_2/Ar ion assistance have a graphitic structure, with C—N π bonds and a low content of C≡N bonds. The films are homogeneous laterally and in depth, with a negligible amount of oxygen and hydrogen. The nitrogen content is limited to [N]/[C] ~ 0.3.

There is a relationship between the contribution of electrons from C and N atoms to the π bonds and the mechanical properties of the films. This is consistent with the arrangement of the basal planes, the softer films consisting of the pileup of weakly interacting graphitic planes and the harder films consisting of a superstructure of interconnected and corrugated basal planes.

The superstructure depends on the growth parameters, mainly on the mixture of bombarding ions and their energy. In particular, films with a similar nitrogen content grown with different N_2/Ar gas mixtures exhibit different mechanical properties and charge distributions in the π bonds.

The hardening mechanism for graphitic films containing more than 70% carbon atoms with sp^2 hybridization seems to be cross-linking of graphitic planes. For carbon nitride films grown with dominant nitrogen assistance the linking sites are nitrogen atoms. For films with a very low nitrogen content grown with dominant Ar ion assistance, the linking sites are carbon sp^3 hybrids. Promotion of both linking sites is competitive and is not obtained simultaneously.